Available online at www.sciencedirect.com
SCIENCE DIRECT®
ELSEVIER
Nuclear Instruments and Methods in Physics Research A 543 (2005) 102–109
NUCLEAR INSTRUMENTS & METHODS IN PHYSICS RESEARCH Section A
www.elsevier.com/locate/nima

Imaging techniques for a high-power THz free electron laser

V.S. Cherkassky[a], B.A. Knyazev[a,b,*], V.V. Kubarev[b], G.N. Kulipanov[b], G.L. Kuryshev[c], A.N. Matveenko[b], A.K. Petrov[d], V.M. Popik[b], M.A. Scheglov[b], O.A. Shevchenko[b], N.A. Vinokurov[b]

[a]*Novosibirsk State University, Novosibirsk 630090, Russian Federation*
[b]*Budker Institute of Nuclear Physics SB RAS, Lavrentiev Av.11, Novosibirsk 630090, Russian Federation*
[c]*Institute of Semiconductor Physics SB RAS, Novosibirsk 630090, Russian Federation*
[d]*Institute of Chemical Kinetics and Combustion SB RAS, Novosibirsk 630090, Russian Federation*

Available online 14 March 2005

Abstract

Two imaging techniques based on the thermal effect have been developed and implemented for recording images using radiation of a high-power terahertz free electron laser. The techniques were applied for the visualization of images in experiments on classical optics, as well as in a holographic experiment.

PACS: 41.60.Cr; 85.60.G; 87.50.Hj

Keywords: Terahertz emission; Infrared detectors; Free electron laser

1. Introduction

Imaging in the terahertz spectral range is a subject of special interest for many applications such as medicine, biology, industry, custom control, and other applications. Recently developed methods for terahertz imaging are based on the employment of the low-power THz sources with a narrowband or wideband spectrum. Due to a low power of these sources, the visualization of images requires the employment of rather sophisticated detectors, and, in most cases, recording of an image requires plenty of time. High power of our laser enables application for the visualization of laser radiation the methods, which, probably, sometime were used for intense visible and NIR radiation, but were never previously employed in the terahertz range. We employed for the visualization, two methods based on the thermal effect of intense terahertz radiation. Now, the Novosibirsk high-power free-electron laser based on microtron-recuperator generates electromagnetic radiation in the wavelength range 120–180 μm as a continuous

*Corresponding author. Budker Institute of Nuclear Physics SB RAS, Lavrentiev Av.11, Novosibirsk 630090, Russian Federation. Tel. +7 3832 394541.
E-mail address: B.A.Knyazev@inp.nsk.su (B.A. Knyazev).

0168-9002/$ - see front matter © 2005 Elsevier B.V. All rights reserved.
doi:10.1016/j.nima.2005.01.122

sequence of 50-ps pulses following with the repetition rate of 5.6 MHz at the average power up to 200 W (the peak power—0.6 MW), the measured relative line width is 0.003 [1].

2. Visualization with a FIR-NIR converter

This technique, further referred as FNC, employs temperature growing of a thin-film screen exposed to terahertz radiation (Fig. 1). Two-dimensional field of temperature at the screen surface is recorded with a thermograph SVIT, which have a 128×128 InAs focal plain array (FPA) sensitive to the radiation within the spectral range of 2.6–3.1 μm. Thermograph sensitivity at the room temperature is 0.03 °C at the frame frequency up to 40 Hz. In our case, time resolution was restricted by thermal relaxation of the thermoconverter and the frame frequency in the experiments was 10 Hz.

In the first experiments, the carbon paper was used as a thermoconverter. Fig. 1 demonstrates the image of keys hided into a dense paper envelope, which is opaque for visible light but transparent for THz radiation. The other picture is a frame of the video film recorded with the thermograph when the aluminum mask with a set of openings forming the letters "FEL BINP" placed in front of the screen. Moving the mask we observed that characteristic thermal relaxation time for the carbon paper was 1–2 s.

3. Visualization with the thermo-optical detector

The other technique used for the visualization of terahertz images was the Thermo-Optical Detector (TOD). The technique employs the change of the optical length of a medium, which is transparent for probe visible light but is opaque for the terahertz radiation, when the medium is exposed

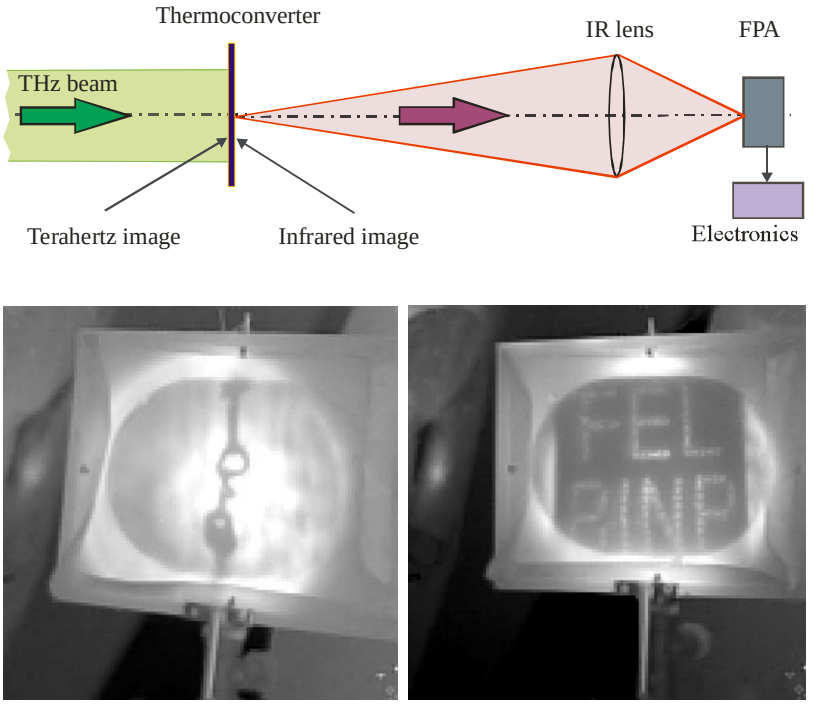

Fig. 1. Schematic layout of the FIR-NIR converter and the snapshots of THz images: keys in the paper envelope and the image recorded when a metal mask with 3-mm holes drilled with a step of 6 mm was placed in front of the thermoconverter.

to terahertz radiation. The change of the optical length within the expose time τ is

$$\Delta S \equiv \frac{\partial S}{\partial t}\tau = \Delta\left[\int_L n(z, T(t))\,\mathrm{d}z\right] \quad (1)$$

where z is the coordinate across the medium slab and T is a local temperature. The difference occurs because of both the thermal expansion and the change of the refraction index for the heated portion of the medium. Corresponding phase shift for a single pass with the accuracy to the members of second-order infinitesimal can be written [2] as

$$\Delta\varphi(x, y) = \frac{\psi}{\lambda} Q(x, y) \quad (2)$$

where $Q(x, y)$ is an real distribution of the specific energy density absorbed in the medium and λ is a wavelength of the probe (visible) radiation. The value

$$\psi[\mathrm{cm}^3/\mathrm{J}] = 2\pi(\beta + \alpha n)/\rho c_p \quad (3)$$

(here $\beta = \mathrm{d}n/\mathrm{d}T$, α, ρ and c_p are a coefficient of thermal expansion, a specific density and a specific heat at constant pressure) is a constant for each optical material. Recording the phase shift, one easy finds the energy density distribution. We have considered several variants of this technique [3]. The variant that was verified experimentally (Fig. 2) employs the interference of two wavefronts of visible coherent light reflected from two surfaces of a parallel-sided (or wedged) glass plate. We used a 20-mW semiconductor laser ($\lambda = 650$ nm) with a lens system as a source of the plane wave. The interference pattern recorded before the expose of the plate to THz radiation was used as a reference one. After that, the plate was exposed to the radiation that is absorbed in the plate (we used both KrF-laser ultraviolet radiation and free electron laser THz radiation) and the diffraction pattern gradually changed because of the thermo-optical effect.

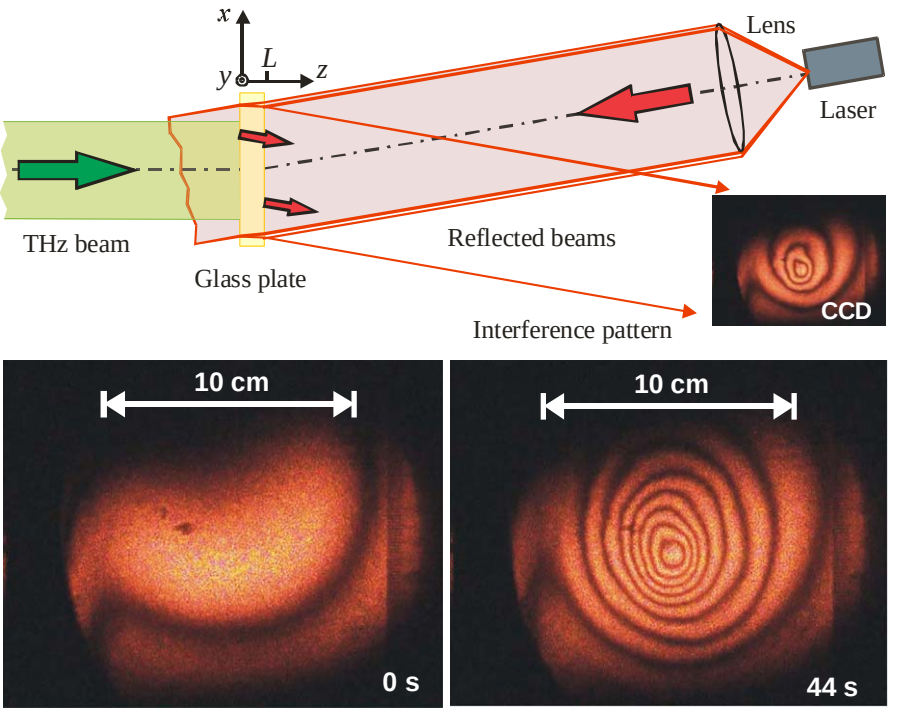

Fig. 2. Schematic layout of the thermo-optical detector (TOD) and the snapshots taken with a digital video camera: the reference interference pattern (on the left) and the image recorded after exposition of the parallel-sided glass plate with THz laser beam during 44 s.

The phase shift of the wave reflected from the rear (exposed to the radiation under study) glass surface obeys Eq. (2). Phase shift at each point $2\Delta\varphi(x,y) = 2[\varphi(\tau) - \varphi(0)]$ is proportional directly to the energy density, deposited into the plate, which can be written as

$$E(x,y;\,t) = \Delta N(x,y;\,t)K. \tag{4}$$

Here ΔN is the fringe shift (generally speaking it is a real but not an integer value) and K is a proportionality factor

$$K = \lambda\rho c_p/2(\beta + \alpha n) \tag{5}$$

where λ is a probe light wavelength and factor 2 appears because the probe wave passes the plate twice. For the inclined reference beam, one needs in addition to take into account, the dip angle.

Factor $K \approx 4.0\,\mathrm{J/fringe\,cm^2}$ for a light glass. Sensitivity of the technique can be increased if one uses a material with higher thermo-optical constant ψ (see Eq. (3)). For example, for PMMA factor $K \approx 0.44\,\mathrm{J/fringe\,cm^2}$ [2]. Thus, the described technique enables direct measurement of the energy density distribution. Time resolution of the technique depends on the expose time and method of the heat sink. Without special cooling and for shot radiation pulses (40-ns pulse of KrF laser) initial interference pattern resumes its original shape in about 1 s after the pulse. For a long expose time, when the heat penetrates deep into the plate, the relaxation time noticeably grows. For the materials with high thermo-optical coefficient and with adequate cooling, one can expect to obtain, for a detector system with a shutter, recording with the frequency of about 10 frames/s. We consider also the possibility to use liquid targets.

The interferograms in Fig. 3 demonstrate application of the TOD to recording THz-laser beam cross-section at the output of the beamline (13 m from the laser output mirror). These interferograms can be interpreted as two frames at the holographic interferometry. Numerical reconstruction of digitally recorded holograms enables to escape the stage of real superimposition of the interferograms and to retrieve the phase difference distribution with a simple digital procedure [4]. It becomes possible because the digital reconstruction of hologram, in contrast to the optical reconstruction, enables to obtain both amplitude and phase of the retrieved wavefront. Methods for interferogram processing are well known and the TOD imaging system working in real time with a high repetition rate does not seem to be impossible. Fig. 3 demonstrates the THz beam cross-section taken with FNC (on the left) and TOD (on the right) techniques. The results reveal reasonable agreement between the

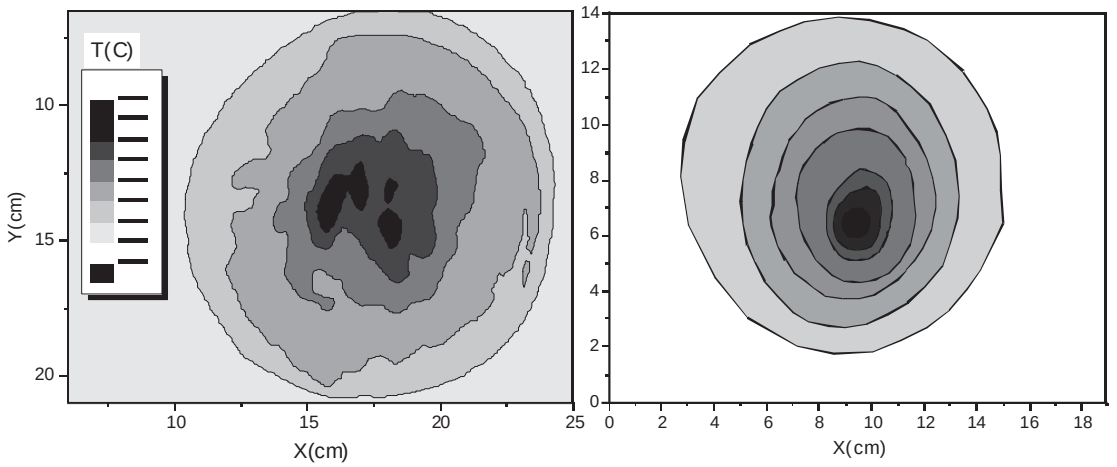

Fig. 3. THz beam cross-sections recorded with FNC (on the left) and TOD. The last image is retrieved from "mirror-reflected" interferogram of Fig. 2, in this case both figures shows the beam cross-section as it is seen at the beamline output.

cross-sections, and their profiles are close to the profile recorded with a pyroelectric transducer.

The TOD technique was also used to visualize (Fig. 4) a fine detailed THz image. To form this image, THz radiation came through the mask in the aluminum plate, shown in Fig. 6, which had the shape of the letter "K" surrounded with an annular aperture. The width of all the apertures was about 3 mm. The mask was placed directly in front of the glass plate and the diffraction effect was negligible.

One can see from Fig. 4 that the interference method enables to obtain undistorted terahertz images when the phase shift is less than 2π. In the opposite case, the interference pattern appears in the image, but the shape of the image is still visible clearly. The image blurs with time due to thermal relaxation. Since the energy distribution of the terahertz beam is close to the Gaussian one, energy deposition in the ring is less than that in the center of the image, and spreading of the ring occurs slower than spreading in the center of the image. Fig. 5 illustrates this fact. It is evident, and special experiments with 20-ns KrF laser corroborated the fact, that for shot pulses one can obtain undistorted images using a thermal screen with an adequate cooling system.

Since measurement of power density, as well as visualization of terahertz radiation, are a subject of high importance for most of the future experiments, we will continue the development of these two techniques and consider other possible methods like the fluorescence board, pyroelectric and Goley-cell matrices and so forth.

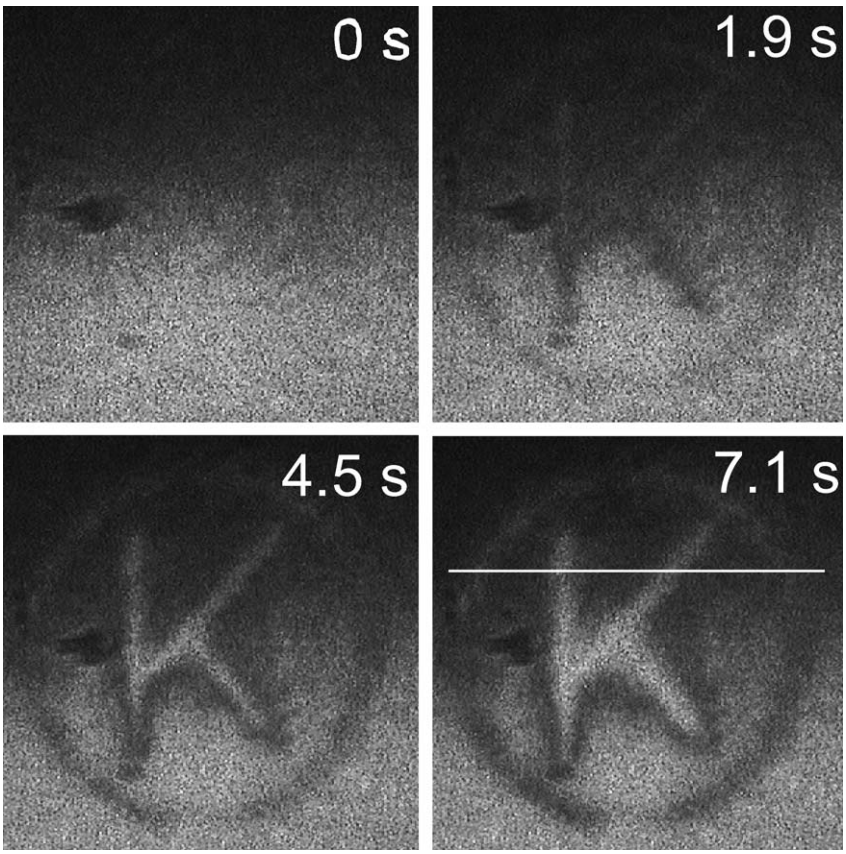

Fig. 4. Sequence of images recorded with the TOD technique (see Fig. 2). THz laser radiation passed through the aperture (see photography in Fig. 6) and was absorbed in the glass plate.

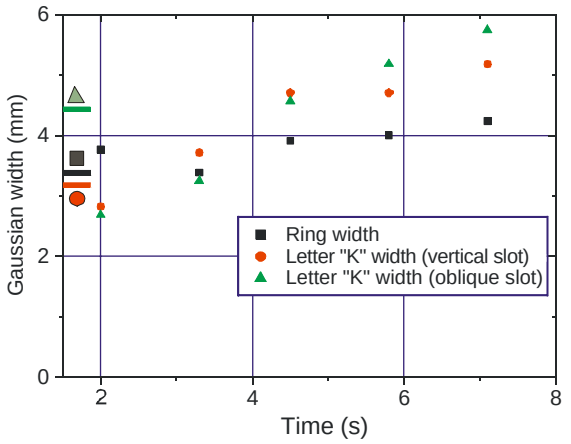

Fig. 5. Gaussian width vs. time for the stripes in the THz image formed with "K and ring" aperture (see Fig. 6) and recorded with the TOD technique. Width profiles were plotted for the trace marked with white line in Fig. 4. The geometrical widths of the slots are shown at the abscissa axis. Some points at the beginning of the curves have very high dispersion due to small noise-to-signal ratio originated from the speckle effect.

4. Classical optic experiments

Photon energy of the submillimeter radiation is about 10 meV. Most of phenomena in this spectral range can be described with excellent precision by the classical optics theory. To demonstrate high transverse and longitudinal coherence of the FEL radiation, we carried out a number of experiments on classical optics.

4.1. Interference and diffraction

The transverse coherence of the free electron laser radiation was clearly demonstrated by classical interference pattern recorded with the thermograph when two large aluminum mirrors, positioned at a small angle, reflected the laser beam on the carbon-paper screen placed at the distance of 180 cm. In the next experiment, we recorded Fresnel diffraction on the mask shown in Fig. 6. In contrast to diffraction experiments in the visible spectral range, for the submillimeter range, characteristic dimension of apertures are to be of a millimeter or a centimeter order of value. Outer diameter of the ring-shape opening in the aperture shown in Fig. 6 is 42 mm. The mask contains seven Fresnel zones for the distance of 180 cm. Since the ring itself contains only one Fresnel zone, its diffraction pattern is a Poisson's spot (right upper picture in Fig. 6). The diffraction pattern of the K-aperture is, as one can expect, contains three main spots corresponding to the three slots. The whole aperture produces more complex diffraction patterns as shown in the right lower frame.

The next diffraction experiment with two circular apertures enables to compare the calculated diffraction pattern with the pattern recorded with that of the thermograph. Two openings were 6 mm in diameter and spaced in horizontal direction at a distance of 14 mm. The screen was placed at the same distance as in the previous experiment. The diffraction pattern at the distance of 108 cm is shown in Fig. 7a. The ratio of initial intensity of THz radiation at the openings was 9:20 (see Fig. 7b).

Experimentally recorded and calculated intensity profiles of the pattern are plotted in Fig. 7c. In the calculation, we took in account the difference in intensities. In the scope of this experiment, the radiation may be considered as completely monochromatic. One can see that the positions and relative intensities perfectly correlate for calculated and recorded peak profiles. We concluded from the numerical simulation that the wavelength of laser radiation in this experiment was 160 μm. This method for the determination of radiation wavelength in the THz spectral range seems to be very simple and reliable, and, obviously, can be used for regular monitoring of THz-laser wavelength.

The peak widths in the experimental profile are wider (and, as a consequence, the fringe visibility is less) than in the calculated one. Apparently, it is a consequence of thermal relaxation over the screen surface. The peak broadening enables to estimate the spatial resolution as 2–3 mm for quasi-CW irradiation. Obviously, using a shutter in the combination with screen cooling allows increasing the spatial resolution.

4.2. Terahertz holography

High radiation intensity of the Novosibirsk free electron laser opens the real opportunity for

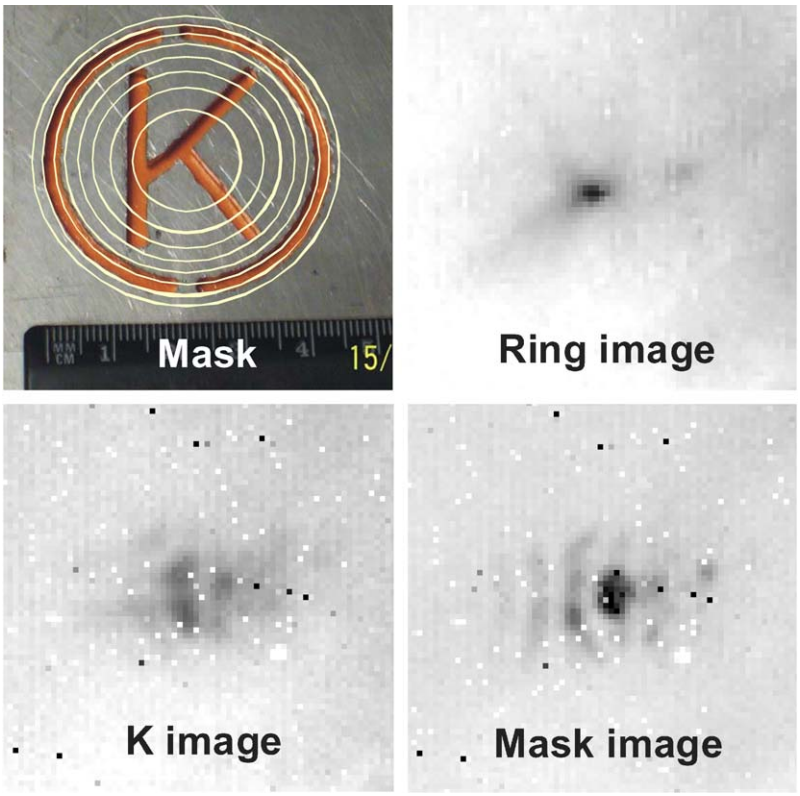

Fig. 6. Photography of the mask with "K and ring" aperture and the diffraction patterns recorded with the thermograph at a distance of 180 cm for partially shaded and completely open aperture. White rings drawn on the mask show the Fresnel zones observing from this distance.

holography in the terahertz spectral range. It does not seem to be possible with the conventional THz sources for at least three reasons. First, most of the sources are not monochromatic. Second, the monochromatic sources have very low intensity, and there are no materials for recording such a radiation. Third, for obtaining an acceptable resolution, a hologram has to have sufficient number of resolving elements [5]. Because of the large wavelength of the THz radiation, this can be done only if the area, where the hologram is recorded, is sufficiently large.

Evidently, our free electron laser has the capability for the development of holography techniques and it will be one of the directions for future experiments. The diffraction patterns presented in Figs. 6 and 7 are already, in fact, the simplest holograms. For example, the letter "K" in the mask in Fig. 6 may be interpreted as an object and the annular aperture plays a role of the reference source. The whole diffraction pattern in this case is a hologram. It is clear that such "lensless Fourier hologram" [5] in Fig. 6 is a very primitive one and has limited number of "interference fringes".

We applied the method of numerical reconstruction of digitally recorded holograms [4] to this hologram and to the "hologram" shown in Fig. 7a. As we expected, the quality of the reconstructed images was very poor, but the reconstruction have demonstrated the main features of such a kind of hologram and the feasibility of holography in the terahertz spectral range. The next goal for our experiments will be recording holograms in the geometry which enables reconstructing THz images with high resolution. Development of terahertz holography may sufficiently enlarge the capability of the terahertz imaging.

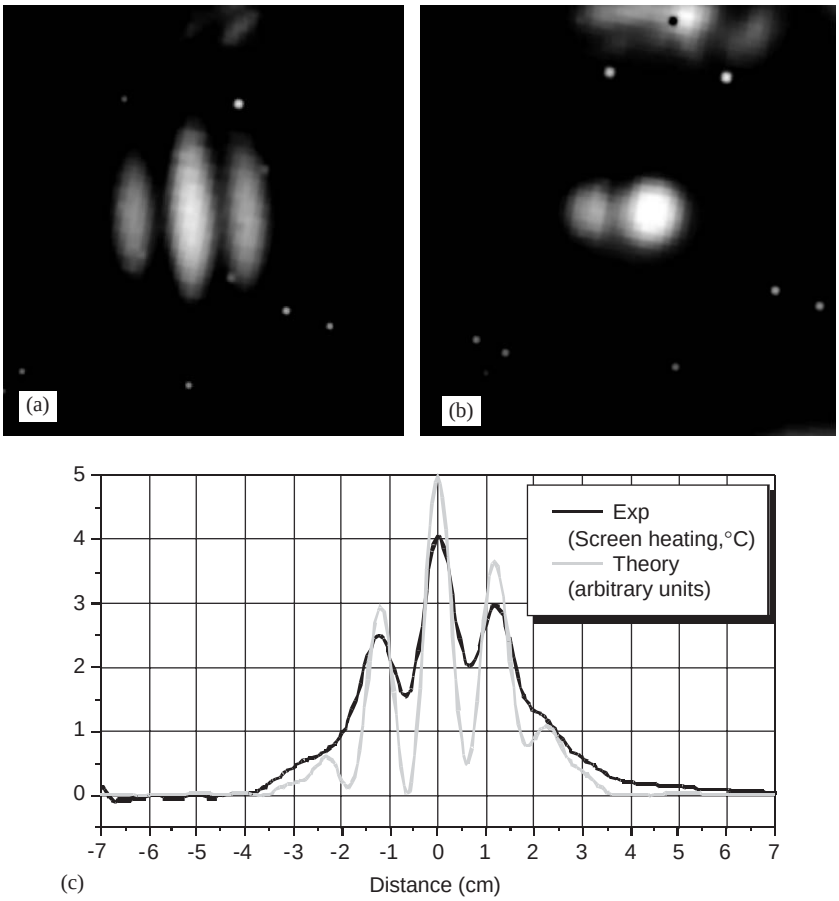

Fig. 7. The diffraction pattern (*a*) produced by two circular apertures (*b*), $\phi = 6\,\text{mm}$, $\Delta = 14\,\text{mm}$, is recorded by the thermograph. The carbon paper screen was placed at a distance of 108 cm. The plot (*c*) shows experimentally observed and theoretically calculated intensity profiles. The theoretical curve was calculated for $\lambda = 160\,\mu\text{m}$.

5. Conclusion

First experiments on the visualization of high-power THz radiation, based on the thermal effects and carried out on the Novosibirsk high power free electron laser facility, have demonstrated its great potentiality for employment in many applications.

Acknowledgement

This work was supported in part by the Siberian Branch of Russian Academy of Science (Grant 174/03). Experimental verification of the thermo-optical detector has been done on the CATRION facility at NSU (reg. #06-06) supported by the Ministry of Education and Science of Russian Federation.

References

[1] E.A. Antokhin, R.R. Akberdin, V.S. Arbuzov, et al., Probl. At. Sci. Technol. 1 (2004) 3.
[2] M.P. Golubev, A.A. Pavlov, Al.A. Pavlov, A.N. Shiplyuk, J. Appl. Mech. Tech. Phys. 44 (2003) 596.
[3] V.S. Cherkassky, B.A. Knyazev, V.V. Kubarev, et al., Proceedings of International Conference IRMMW2004/THz2004, Karlsruhe, Germany, 2004, in print.
[4] U. Schnars, W.P.O. Juptner, Meas. Sci. Technol. 13 (2002) R85.
[5] R.J. Collier, C.B. Burckhardt, L.H. Lin, Optical Holography, Academic Press, New York and London, 1971.